Antiferromagnetic Vortex Core in $Tl_2Ba_2CuO_{6+\delta}$ Studied by Nuclear Magnetic Resonance

K. Kakuyanagi,[1] K. Kumagai,[1] Y. Matsuda,[2] and M. Hasegawa[3]

[1]*Division of Physics, Graduate School of Science, Hokkaido University, Sapporo 060-0810, Japan*
[2]*Institute for Solid State Physics, University of Tokyo, Kashiwanoha 5-1-5, Kashiwa, Chiba 277-8581, Japan*
[3]*Institute of Material Research, Tohoku University, Katahira, Sendai, 980-8577, Japan*

(Received 19 June 2002; published 15 May 2003)

Spatially resolved NMR is used to probe the magnetism in and around vortex cores of nearly optimally doped $Tl_2Ba_2CuO_{6+\delta}$ ($T_c = 85$ K). The NMR relaxation rate T_1^{-1} at the ^{205}Tl site provides direct evidence that the antiferromagnetic (AF) spin correlation is significantly enhanced in the vortex core region. In the core region Cu spins show a local AF ordering with moments parallel to the layers at $T_N = 20$ K. Above T_N the core region is in the paramagnetic state which is a reminiscence of the state above the pseudogap temperature ($T^* \simeq 120$ K), indicating that the pseudogap disappears within cores.

DOI: 10.1103/PhysRevLett.90.197003 PACS numbers: 74.25.Ha, 74.25.Nf, 74.72.Jt, 76.60.–k

In high-T_c cuprates (HTC) the superconductivity with d-wave symmetry appears when carriers are doped into the antiferromagnetic (AF) Mott insulators. It is well established that the strong AF fluctuation plays a crucial role in determining many physical properties. Therefore the relation between superconductivity and magnetism has been a central issue in the physics of HTC. Especially, how the antiferromagnetism emerges when the d-wave superconducting order parameter is suppressed is a fundamental problem in the superconducting state [1,2]. In this respect, the microscopic structure of vortex core, which is a local normal region created by destroying the superconductivity by magnetic field, turns out to be a very interesting subject.

Within the framework of the semiclassical approximation, in which the electron correlation effects are ignored, vortex cores in d-wave superconductors are in the normal metallic state which is the same as the state above T_c, similar to s-wave superconductors [3]. However, recent high resolution scanning tunneling microscopy (STM) experiments have revealed many unexpected properties in the spectrum of vortex cores, which are fundamentally different from these semiclassical d-wave vortex cores [4]. For instance, a checkerboard halo of the local density of states (LDOS) around the core has been reported in $Bi_2Sr_2CaCu_2O_{8+\delta}$ [5]. A new class of theories has pointed out that the strong electron correlation effects change the vortex core structure dramatically. For example, possible competing orders, such as AF [6], staggered flux [7], and stripe [2,8] orderings in and around cores have been discussed. Therefore it is crucial for gaining an understanding of the vortex state of HTC to clarify how the AF correlation and pseudogap phenomena, which characterize the magnetic excitation in the normal state, appear in and around vortex cores.

Despite extensive studies, little is known about the microscopic electronic structure of the vortices, especially concerning the magnetism. The main reason for this is that STM experiments do not directly reflect the magnetism. Neutron scattering experiments on $La_{2-x}Sr_xCuO_4$ have reported that an applied magnetic field enhances the AF correlation in the superconducting state [9]. However, the relation between the observed AF ordering and the magnetism within vortex cores is not clear, because the neutron experiments lack spatial resolution. Recent μSR experiments on underdoped $YBa_2Cu_3O_{6.5}$ have reported the presence of static magnetism in the vortex core region [10], but the detailed nature of this magnetism is still not clear.

Recent experimental [11–13] and theoretical [14] NMR studies have established that the frequency dependence of the spin-lattice relaxation rate T_1^{-1} in the vortex state serves as a probe for the low energy excitation spectrum which can resolve *different spatial regions of the vortex lattice*. Unfortunately, up to now, all of these spatially resolved NMR measurements have been carried out at the planar ^{17}O sites [11–13], at which the AF fluctuations are filtered due to the location of O atoms in the middle of neighboring Cu atoms with antiparallel spins [15].

In this Letter we provide local information on the AF correlation in the different regions of the vortex lattice extending the measurements to the vortex core region, by performing spatially resolved NMR imaging experiments on ^{205}Tl nuclei in nearly optimally doped $Tl_2Ba_2CuO_{6+\delta}$. This attempt is particularly suitable for the above purpose because T_1^{-1} at the Tl site, $^{205}T_1^{-1}$, can monitor AF fluctuations sensitively. Quite generally, $1/T_1$ is expressed in terms of the dynamical susceptibility as $\frac{1}{T_1} = \frac{\gamma_n k_B T}{2\mu_B^2} \sum_q |A_q|^2 \frac{\mathrm{Im}\chi(q,\omega_0)}{\omega_0}$, where γ_n is the nuclear gyromagnetic ratio, A_q is the hyperfine coupling between nuclear and electronic spins, and ω_0 is the Larmor frequency. Because Tl atoms are located just above the Cu atoms and there exist large transferred hyperfine interactions between Tl nuclei and Cu spin moments through apical oxygen, Tl sees the full wavelength spectrum of Cu magnetic spin fluctuation; $^{205}T_1$ is dominated by $\chi(\boldsymbol{q})$ at $\boldsymbol{q} = (\pi, \pi)$, i.e., AF fluctuations. This should

be contrasted to the O sites at which $\chi(\boldsymbol{q})$ is dominated by uniform fluctuations at $\boldsymbol{q} = (0, 0)$.

NMR measurements were carried out on the c-axis oriented polycrystalline powder of high quality $Tl_2Ba_2CuO_{6+\delta}$ ($T_c = 85$ K) in the external field ($H_0 = 2.1$ T) along the c axis. The ^{205}Tl spin echo signals were obtained by a pulse NMR spectrometer. The spectra were obtained by convolution of the respective Fourier-transform spectra of the spin echo signals measured with an increment of 50 kHz. A very sharp spectrum ($\sim$50 kHz) above T_c becomes broad below T_c due to the development of vortices. The solid lines in Fig. 1 and in the lower inset depict the NMR spectra at 5 K and 20 K, respectively. A clear asymmetric pattern of the NMR spectrum, which originates from the local field distribution associated with the vortex lattice is observed below the vortex lattice melting temperature ($\sim$60 K at H_0) [16]. The local field profile in the vortex state is given by approximating $H_{\rm loc}(\mathbf{r})$ with the London result,

$$H_{\rm loc}(\boldsymbol{r}) = H_0 \sum_G \exp(-i\boldsymbol{G}\cdot\boldsymbol{r}) \frac{\exp(-\xi_{ab}^2 \boldsymbol{G}^2/2)}{1 + \boldsymbol{G}^2 \lambda_{ab}^2}, \quad (1)$$

where $\boldsymbol{G}$ is a reciprocal vector of the vortex lattice, $|\,\boldsymbol{r}\,|$ is the distance from the center of the core, ξ_{ab} is the in-plane coherence length, and λ_{ab} is the in-plane penetration length. The thin solid lines in Fig. 1 depict the histogram at a particular local field which is given by the local field distribution $f(H_{\rm loc}) = \int_\Omega \delta[H_{\rm loc}(\boldsymbol{r}) - H_{\rm loc}] d^2\boldsymbol{r}$ in Eq. (1) assuming the square vortex lattice, where Ω is the magnetic unit cell. The upper inset shows the image of the field distribution in the vortex lattice. In the prefect vortex lattice and without magnetism within cores which will be discussed later, the histogram shows the low and high frequency cutoffs at the center of the vortex lattice (point C) and at the center of cores (point A), respectively, and shows a peak at the field corresponding to the saddle point (point B). This characteristic spectrum (Redfield pattern) demonstrates that the NMR frequency depends on the position of the vortex lattice. We therefore can obtain the spatially resolved information of the low energy excitation by analyzing the frequency distribution of the corresponding NMR spectrum.

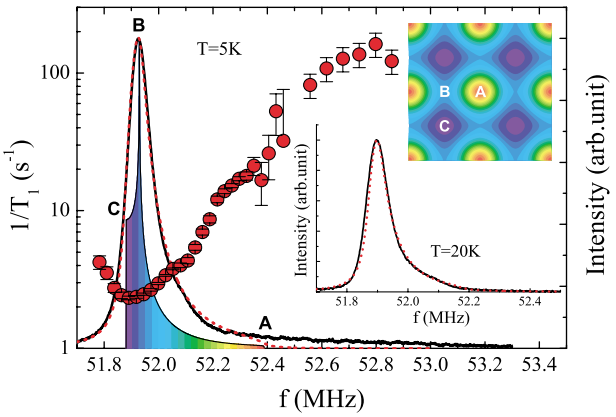

FIG. 1 (color). Main panel: ^{205}Tl-NMR spectrum (solid line) at 5 K. The intensity is plotted in a linear scale. The thin solid lines depict the histogram at particular local fields obtained from Eq. (1). In the calculation we used $\xi_{ab} = 18$ Å and $\lambda_{ab} = 1700$ Å. The red dotted line represents the simulation spectrum convoluted with Lorentzian broadening function. The red filled circles show the frequency dependence of T_1^{-1} at the Tl site. For details, see the text. Lower inset: ^{205}Tl-NMR spectrum (solid line) and the simulation spectrum (red dotted line) at 20 K. In the calculation we used $\xi_{ab} = 18.5$ Å and $\lambda_{ab} = 2000$ Å. Upper inset: the image of the field distribution in the vortex square lattice; center of vortex core (A), saddle point (B), and center of vortex lattice (C).

We first discuss the observed NMR spectra. The real spectrum broadens due to the imperfect orientation of the power and distortion of the vortex lattice. The red dotted lines in Fig. 1 and the lower inset represent the simulation spectra in which the Lorentzian broadening function, $f(H_{\rm loc}) = \sigma/(4H_{\rm loc}^2 + \sigma^2)$, is convoluted to Redfield pattern using $\sigma = 42$ kHz. The theoretical curve reproduces the data well in the whole frequency range at $T = 20$ K (inset). On the other hand, the spectrum at 5 K shows significant broadening at the high frequency region (core region), while it can be well fitted below 52.1 MHz (main panel). The filled circles in Fig. 2 display the linewidth at the high frequency tail, Δf, which is defined as a difference between the frequency at the peak intensity and the frequency at which the intensity becomes 1% of the peak. For the comparison, the linewidth calculated from the simulation spectra with the Lorentzian broadening function is plotted by the dashed line. At high temperatures Δf agrees well with the calculation, while below 20 K it becomes much larger. We also plot δf which represents the linewidth at the half intensity (open circles). The fact

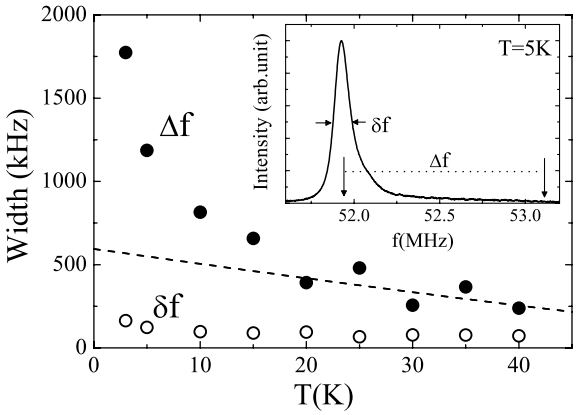

FIG. 2. The linewidths of the ^{205}Tl-NMR spectrum plotted as a function of T. Δf (filled circles) indicates the linewidth determined by the frequency at which the intensity becomes 1% of the peak. The dashed line represents the linewidth calculated from the simulation spectrum without taking into account the core magnetism. Open circles represent δf which is defined as the linewidth at the half intensity. The inset shows the spectrum at 5 K and the definition of Δf and δf.

that δf changes little below 20 K confirms that the line broadening occurs only in the high frequency core region. In μSR experiments, the high frequency tail was attributed to the static magnetism around cores, which causes additional broadening [10]. It should be noted that because of large transfer hyperfine coupling between Tl nuclei and Cu moment, the broadening of the Tl-NMR spectrum associated with the static magnetism is more pronounced than that of the μSR spectrum. Therefore the observed broadening below $\sim$20 K is naturally explained by the appearance of static magnetism within cores below $\sim$20 K. To obtain deep insight into this phenomenon, the measurements of T_1 are crucial.

For ^{205}Tl with nuclear spin $I = 1/2$, the recovery curve of the nuclear magnetization $M(t)$ fits well to a single exponential relation, $R(\tau) = [M(\infty) - M(\tau)]/M(\infty) = \exp(-\tau/T_1)$ in the normal state. In the vortex state, on the other hand, the feature of the recovery curves is strongly position dependent as shown in Fig. 3. The spin echo intensities are measured as a function of τ after saturation pulses. Then the nuclear magnetization recovery curves are obtained from each frequency component of the Fourier transform spectra. We obtained the data set of the recovery intensity for each frequency point at the 28 kHz interval with a Gaussian weight function of $\sigma = 10$ kHz. There are two distinct features. First, the decay time at cores is much faster than at saddle points. Second, while the recovery curves show the single exponential at the saddle point, they show a root exponential dependence at the core region as shown in the inset of Fig. 3. We discuss this $\sqrt{\tau}$ dependence later. In what follows, we define T_1 as the time required for the nuclear magnetization to decay by a factor $1/e$, in order to define T_1 uniquely for either decay curve.

The red filled circles in Fig. 1 show the frequency dependence of $^{205}T_1^{-1}$. On scanning from outside into cores, $^{205}T_1^{-1}$ increases rapidly after showing a minimum

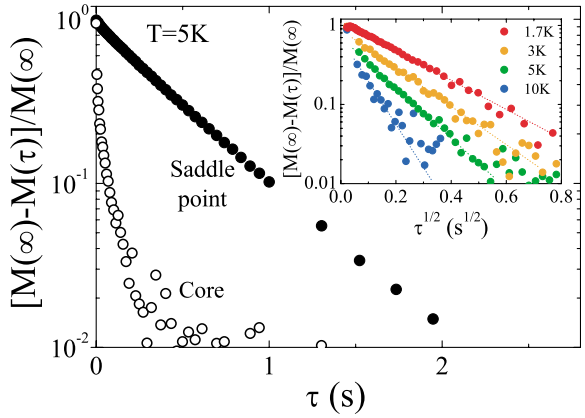

FIG. 3 (color). Recovery curves of nuclear magnetization of ^{205}Tl as a function of time, τ. The filled and open circles represent the data at the saddle points and at vortex cores, respectively. The inset shows the recovery curves at cores as a function of $\sqrt{\tau}$ at several temperatures.

near saddle points. The magnitude of $^{205}T_1^{-1}$ in the core region is almost 2 orders of magnitude larger than that near the saddle point. This large enhancement of $^{205}T_1^{-1}$ is in striking contrast to $^{17}T_1^{-1}$ at ^{17}O sites reported in $YBa_2Cu_3O_7$ [11,12] and $YBa_2Cu_4O_8$ [13], in which the enhancement of $^{17}T_1^{-1}$ at the core region is 2–3 times at most and has been attributed to LDOS produced by a Doppler shift of the quasiparticle energy spectrum by supercurrents around the vortices [17]. It should be noted that the LDOS effect is absent in $^{205}T_1^{-1}$, because there are no conduction electrons at the ^{205}Tl site. Therefore, the remarkable enhancement of $^{205}T_1^{-1}$ provides direct evidence that *the AF correlation is strongly enhanced near the vortex core region* [18]. The decrease of $^{205}T_1^{-1}$ well outside the core when going from point C to B was also reported in $^{17}T_1^{-1}$ [12,13].

Figures 4(a) and 4(b) depict the T dependences of $(^{205}T_1T)^{-1}$ and $^{205}T_1^{-1}$ within cores (filled circles) and at the frequency corresponding to saddle points (open circles), respectively. In these figures, $^{205}T_1^{-1}$ within cores, $(^{205}T_1^{\rm core})^{-1}$, were determined with using integrated intensities over the high frequency region beyond point A. From high temperatures down to about 120 K, $(^{205}T_1T)^{-1}$ obeys the Curie-Weiss law, $(^{205}T_1T)^{-1} \propto 1/(T + \theta)$. The lowest T at which this law holds is conveniently called the pseudogap temperature T^*. Below T^*, $(^{205}T_1T)^{-1}$ decreases rapidly without showing any anomaly associated with the superconducting transition at T_c, similar to other HTC [15].

The T dependence of $(^{205}T_1^{\rm core})^{-1}$ contains some key features for understanding the core magnetism. The first important signature is that $1/^{205}T_1^{\rm core}$ exhibits a sharp peak at $T = 20$ K, which we label as T_N for future reference [Fig. 4(b)]. Below T_N $(^{205}T_1^{\rm core})^{-1}$ decreases rapidly with decreasing T. There are two possible origins for this

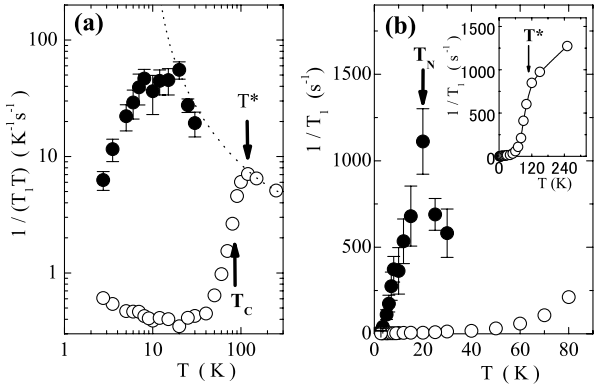

FIG. 4. (a) T dependence of $(^{205}T_1T)^{-1}$. (b) T dependence of $^{205}T_1^{-1}$ at low temperatures (main panel) and at high temperatures (inset). The filled and open circles represent the data at vortex cores and at saddle points, respectively. $T^* \simeq 120$ K is the pseudogap temperature. The dotted line represents the Curie-Weiss law which is determined above T^*. In (b), T_N is the temperature at which $^{205}T_1^{-1}$ at the core exhibits a sharp peak.

peak. One is the reappearance of the pseudogap and the other is the occurrence of a local static AF [or spin density wave (SDW)] ordering in the core region. Generally T_1^{-1} shows a sharp peak when the AF ordering occurs. The fact that the sharp peak of $(^{205}T_1^{\rm core})^{-1}$ is observed at T_N while $1/T_1$ at the saddle points shows neither a peak nor broad maximum at T^* as shown in the inset of Fig. 4(b) excludes the possibility of pseudogap, supporting the AF ordering. Moreover, as shown in Fig. 2, broadening of the NMR spectrum starts at ~20 K, which coincides with T_N. This fact gives additional strong evidence on AF ordering. We also point out that the appearance of the local AF ordering is also consistent with the $\sqrt{\tau}$ dependent nuclear magnetization decay curve shown in the inset of Fig. 3. In fact, the $\sqrt{\tau}$ dependence has been observed when the microscopic imhomogeneous distribution of T_1^{-1} due to strong magnetic scattering centers is present [20]. On the basis of these results, we are led to conclude that the local AF ordering takes place in the core region at $T_N = 20$ K; *T_N corresponds to the Néel temperature within the core*. This AF ordering is consistent with the prediction of recent theories based on the *t-J* and SO(5) models [6]. The present results also should be distinguished from those of the neutron scattering experiments on $La_{2-x}Sr_xCuO_4$ [9], in which the static SDW coexists with superconductivity even in zero field just below T_c. In the present compound, on the other hand, we do not observe such a static SDW ordering and the vortex core region is in the paramagnetic state in a wide T region between T_c and T_N.

As discussed before, the broadening occurs only at high frequencies. This fact indicates that *the AF spins are oriented parallel to the* CuO_2 *layers*. This follows by observing that the broadening should occur at both high and low frequency sides if the AF ordering occurs perpendicular to the layers, because in this case the direction of the alternating transferred hyperfine fields is parallel and antiparallel to the applied field. Using the hyperfine coupling constant, $A_{\rm hf} = 65$ kOe/μ_B, the magnetic moments induced within the core are estimated to be $\sim 0.1\mu_B$ at H_0. The detailed analysis will be published elsewhere.

The second important signature for the core magnetism is that, as shown by the dotted line in Fig. 4(a), $(^{205}T_1^{\rm core}T)^{-1}$ above T_N nearly lies on the Curie-Weiss law line extrapolated above T^*. This fact indicates that the vortex core region appears to be *in the paramagnetic state which is a reminiscence of the state above T^*; the pseudogap is absent in the core region*. This result seems to be inconsistent with the recent theories which predict local orbital currents, in which the pseudogap phenomenon within cores is assumed [6].

Summarizing the salient features of spatially resolved NMR results in the vortex lattice, (i) the NMR spectrum near the core region broadens below $T = 20$ K (Figs. 1 and 2). (ii) Upon approaching the vortex core, $(^{205}T_1)^{-1}$ is strongly enhanced (Fig. 1). (iii) Near the core region, the NMR recovery curves show the $\sqrt{\tau}$ dependence (Fig. 3). (iv) $(^{205}T_1^{\rm core})^{-1}$ exhibits a sharp peak at $T = 20$ K (Fig. 4). All of these results provide direct evidence that in the vortex core region the AF spin correlation is extremely enhanced and that the paramagnetic-AF ordering transition of the Cu spins takes place at $T_N = 20$ K. We also find the pseudogap disappears within the core. The present results offer a new perspective on how the AF vortex core competes with the *d*-wave superconductivity.

We acknowledge helpful discussions with M. Franz, M. Imada, J. Kishine, K. Machida, D. K. Morr, M. Ogata, S. H. Pan, M. Takigawa, A. Tanaka, Z. Tesanović, and O. M. Vyaselev.

[1] S. C. Zhang, Science **275**, 1089 (1997).
[2] Y. Zhang, E. Demler, and S. Sachdev, Phys. Rev. B **66**, 094501 (2001), and references therein.
[3] N. Schopohl and K. Maki, Phys. Rev. B **52**, 490 (1995); M. Ichioka *et al.*, Phys. Rev. B **53**, 15 316 (1996).
[4] I. Maggio-Aprile *et al.*, Phys. Rev. Lett. **75**, 2754 (1995); S. H. Pan *et al.*, *ibid.* **85**, 1536 (2000).
[5] J. E. Hoffman *et al.*, Science **295**, 466 (2002).
[6] D.P. Arovas *et al.*, Phys. Rev. Lett. **79**, 2871 (1997); J. H. Han and D. H. Lee, *ibid.* **85**, 1100 (2000); Jian-Xin Zhu and C. S. Ting, *ibid.* **87**, 147002 (2001); Jian-Xin Zhu *et al.*, *ibid.* **89**, 067003 (2002); M. Ogata, Int. J. Mod. Phys. B **13**, 3560 (1999); H. Tsuchiura *et al.*, cond-mat/0302030.
[7] J. Kishine *et al.*, Phys. Rev. Lett. **86**, 5365 (2001); Q. H. Wang *et al.*, *ibid.* **87**, 167004 (2001).
[8] M. Takigawa *et al.*, Phys. Rev. Lett. **90**, 047001 (2003).
[9] B. Lake *et al.*, Science **291**, 1759 (2001); B. Lake *et al.*, Nature (London) **415**, 299 (2002); B. Khaykovich *et al.*, Phys. Rev. B **66**, 014528 (2002).
[10] R. I. Miller *et al.* Phys. Rev. Lett. **88**, 137002 (2002).
[11] N. J. Curro *et al.*, Phys. Rev. B **62**, 3473 (2000).
[12] V. F. Mitrovic *et al.*, Nature (London) **413**, 501 (2001); V. F. Mitrovic *et al.*, cond-mat/0202368.
[13] K. Kakuyanagi *et al.*, Phys. Rev. B **65**, 060503 (2002).
[14] M. Takigawa *et al.*, Phys. Rev. Lett. **83**, 3057 (1999); R. Wortis *et al.*, Phys. Rev. B **61**, 12 342 (2000); D. K. Morr and R. Wortis, Phys. Rev. B **61**, R882 (2000); D. K. Morr, Phys. Rev. B **63**, 214509 (2001); Y. Chen *et al.*, cond-mat/0302114.
[15] V. Barzykin and D. Pines, Phys. Rev. B **52**, 13 585 (1995).
[16] We stress the importance of the measurements under the field cooling condition in the vortex lattice phase to observe the asymmetric field profile.
[17] G. E. Volovik, JETP Lett. **58**, 469 (1993).
[18] We note that $(^{205}T_1^{\rm core})^{-1}$ is 2 orders of magnitude larger than that expected solely from vortex vibration at all temperatures (see Fig. 2 in Ref. [19]).
[19] L. N. Bulaevskii *et al.*, Phys. Rev. Lett. **71**, 1891 (1993).
[20] M. R. McHenry *et al.*, Phys. Rev. B **5**, 2958 (1972).